Residual Elimination Algorithm Enhancements to Improve Foot Motion Tracking During Forward Dynamic Simulations of Gait

Jennifer N. Jackson[1]
Department of Biomedical Engineering,
University of Florida,
Gainesville, FL 32611;
Functional and Applied Biomechanics Section,
Rehabilitation Medicine Department,
National Institutes of Health,
Bethesda, MD 20892

Chris J. Hass
Department of Applied Physiology
and Kinesiology,
University of Florida,
Gainesville, FL 32611

Benjamin J. Fregly[2]
Department of Mechanical
and Aerospace Engineering,
University of Florida,
Gainesville, FL 32611;
Department of Biomedical Engineering,
University of Florida,
Gainesville, FL 32611
e-mail: fregly@ufl.edu

*Patient-specific gait optimizations capable of predicting post-treatment changes in joint motions and loads could improve treatment design for gait-related disorders. To maximize potential clinical utility, such optimizations should utilize full-body three-dimensional patient-specific musculoskeletal models, generate dynamically consistent gait motions that reproduce pretreatment marker measurements closely, and achieve accurate foot motion tracking to permit deformable foot-ground contact modeling. This study enhances an existing residual elimination algorithm (REA) Remy, C. D., and Thelen, D. G., 2009, "Optimal Estimation of Dynamically Consistent Kinematics and Kinetics for Forward Dynamic Simulation of Gait," ASME J. Biomech. Eng., **131**(3), p. 031005) to achieve all three requirements within a single gait optimization framework. We investigated four primary enhancements to the original REA: (1) manual modification of tracked marker weights, (2) automatic modification of tracked joint acceleration curves, (3) automatic modification of algorithm feedback gains, and (4) automatic calibration of model joint and inertial parameter values. We evaluated the enhanced REA using a full-body three-dimensional dynamic skeletal model and movement data collected from a subject who performed four distinct gait patterns: walking, marching, running, and bounding. When all four enhancements were implemented together, the enhanced REA achieved dynamic consistency with lower marker tracking errors for all segments, especially the feet (mean root-mean-square (RMS) errors of 3.1 versus 18.4 mm), compared to the original REA. When the enhancements were implemented separately and in combinations, the most important one was automatic modification of tracked joint acceleration curves, while the least important enhancement was automatic modification of algorithm feedback gains. The enhanced REA provides a framework for future gait optimization studies that seek to predict subject-specific post-treatment gait patterns involving large changes in foot-ground contact patterns made possible through deformable foot-ground contact models.*
[DOI: 10.1115/1.4031418]

Keywords: gait, walking, residual elimination algorithm, optimization, forward dynamic simulation, biomechanics

Introduction

Clinical conditions affecting the neuromusculoskeletal system (e.g., osteoarthritis [1], stroke [2], Parkinson's disease [3]) can significantly limit walking function and are primary causes of disability among U.S. adults. Such conditions cost the U.S. economy billions of dollars annually in medical care and lost productivity [4]. Furthermore, as walking ability diminishes, quality of life decreases and the risk of death increases [5–7], making restoration of walking function a critical problem for public health. Current treatment design methods for these conditions rely heavily on subjective clinical judgment and have been largely ineffective at restoring normal walking function [8]. This observation suggests that new treatment design methods are necessary to address the unique challenges posed by these clinical conditions.

Computational walking models employing multibody dynamic modeling methods could augment current treatment design methods by permitting objective and personalized exploration of different treatment options prior to making the final decision. For example, such models could be used to evaluate whether gait modification is likely to achieve the same reduction in peak knee adduction moment as would high tibial osteotomy surgery for a specific patient. To predict a patient's post-treatment walking function starting from the patient's pretreatment walking data, a computational model should ideally fulfill at least seven requirements. First, it should be three-dimensional, since clinical problems are often related to motions and loads outside the sagittal plane (e.g., the knee adduction moment in knee osteoarthritis [9]). Second, it should be full body including the arms, since modeling the arms is necessary to predict walking motions for clinical situations where the arms naturally move and affect body dynamics. Third, it should be patient-specific, at a minimum calibrating joint positions and orientations along with segment masses, mass centers, and moments of inertia to the patient's pretreatment movement data [10]. Fourth, it should be dynamically consistent, meaning that the six full-body dynamics equations are satisfied exactly rather than to some arbitrarily defined level. Fifth, it should reproduce pretreatment experimental marker data closely, providing a realistic starting point for subsequent optimizations that predict new gait patterns. Sixth, it should also reproduce pretreatment experimental ground reaction forces and moments closely using a deformable foot-ground contact model, thereby permitting prediction of new gait patterns that require new foot-ground contact patterns (e.g., going from toe striking to heel striking). Finally, it should predict clinically important quantities that could aid in the treatment design process (e.g., post-treatment walking speed and symmetry).

[1]The majority of the research was completed at the University of Florida.
[2]Corresponding author.
Manuscript received January 23, 2015; final manuscript received August 19, 2015; published online September 16, 2015. Assoc. Editor: Paul Rullkoetter.

A number of research groups have made important strides in this area, achieving some but not all of these requirements (Table 1). Many studies have used three-dimensional walking models [11–21]. However, only a subset of those studies either included modeling the motion of the arms [12–16,20] or were dynamically consistent [11,13,16–18], with very few satisfying both criteria [13,16], making prediction of clinically realistic walking motions difficult. Many studies used deformable foot-ground contact models [11,17,18,22–27], which permit prediction of new foot paths. However, only a small number of those studies predicted novel walking motions for which no experimental data were available [18,23,25–27]. Even fewer studies generated walking predictions that have potential clinical utility [15,22,24,27]. Rarely did studies calibrate joint and inertial parameter values to the subject's movement data [15]. Omitting calibration of joint parameters (i.e., joint positions and orientations in their segment frames) can have a significant effect on simulated joint moments [28]. Thus, new methods need to be developed that cover the broadest possible spectrum of these requirements.

This study describes the development of a computational algorithm that fulfills the first five requirements listed above, providing a stepping stone for future efforts that will seek to fulfill all seven requirements. The algorithm is a natural extension of the "Residual Elimination Algorithm" (REA) published by Remy and Thelen in 2009 [13], which generates forward dynamic walking simulations that closely reproduce experimental gait data. While that algorithm tracks marker positions closely using a dynamically consistent three-dimensional walking model, it does not permit calibration of model parameter values, nor are foot marker motions tracked as closely as necessary for future inclusion of a deformable foot-ground contact model. To calibrate model parameter values and achieve better tracking of foot markers, we developed an enhanced REA that adjusted: (1) marker weights, (2) tracked acceleration curves, (3) feedback gains, and (4) joint and inertial parameter values. While the marker weights are adjusted manually, each of the remaining changes is automated within the enhanced REA framework. We explored each modification individually and in combinations to determine which ones yielded the lowest foot and overall marker tracking errors. In addition, since greater back flexibility may help the model achieve better marker tracking, we also explored the potential benefit of using a two-joint back model with and without additional degrees of freedom (DOFs).

Methods

Enhanced REA Gait Model. We used a modified version of an existing three-dimensional full-body dynamic skeletal model (i.e., no muscles included) to develop and evaluate our enhanced REA. The existing skeletal model possesses 14 segments and 27 DOFs [15]. The ankles were modeled as two non-intersecting pin joints, the knees as pin joints, the hips as ball-and-socket joints, the back as a ball-and-socket joint at approximately the L4-L5 level, the shoulders as universal joints, and the elbows as pin joints, with the pelvis being connected to ground via a 6 DOF joint that allows translation and rotation of the model in the laboratory reference frame.

We made two modifications to this model to explore how increased model complexity affects marker tracking errors. First, to accommodate nonsagittal arm motion, we added internal/external rotational DOFs to both shoulders, thereby increasing the number of DOFs to 29 (Fig. 1(*a*)). Second, we split the back into two segments by adding a second ball-and-socket joint at the T8-T9 level, further increasing the number of DOFs to 32 (Fig. 1(*b*)). The additional shoulder DOFs were used in all evaluations, while the additional back DOFs were treated three ways to explore how back flexibility affected the results: (1) upper back joint locked so that all motion occurred in the lower back joint (29 DOFs), (2) upper back joint prescribed to move identically to lower back joint (29 DOFs), and (3) upper back joint free to move independently from lower back joint (32 DOFs). To illustrate the second case, when the lower back is extended by three degrees, the upper back will be extended by three degrees relative to the lower back segment. Our model has two more DOFs than the model used to develop the original REA [13] since we modeled the ankle as two nonintersecting and nonorthogonal pin joints rather than as a single pin joint. We derived the equations of motion for each model using Autolev symbolic manipulation software (Motion Genesis, Palo Alto, CA). All optimizations were performed using Matlab's (The Mathworks, Natick, MA) nonlinear least squares algorithm with forward finite differences used to calculate gradients.

Enhanced REA Development. The original REA [13] finds new initial conditions and generalized accelerations that produce a dynamically consistent walking motion (i.e., fictitious pelvis residual loads eliminated) while tracking experimentally measured

Table 1 Summary of published studies that use computational walking models and their fulfillment of requirements for maximizing potential clinical utility. Only walking models published between 2000 and the present were included. When related papers from the same lab appear in different years, only one of those papers was included as being representative.

Study	Gait model dimensionality	Model with arms included?	Joint and inertial parameters calibrated?	Dynamically consistent model?	Experimental motion tracked?	Deformable foot-ground contact model?	Novel gait motion predicted?	Clinically useful information predicted?
Jansen et al. (2014) [20]	3D	Yes	No	No	Joints	No	No	No
Allen et al. (2013) [11]	3D	No	No	Yes	Joints	Yes	No	No
Fey et al. (2013) [22]	2D	No	No	Yes	Joints	Yes	No	Yes
Miller et al. (2013) [27]	2D	No	No	Yes	Joints	Yes	Yes	Yes
Thompson et al. (2013) [21]	3D	No	No	No	Joints	No	No	No
Ackermann and van den Bogert (2012) [23]	2D	No	No	Yes	Joints	Yes	Yes	No
Higginson et al. (2011) [19]	3D	No	No	No	Joints	No	No	No
van den Bogert et al. (2011) [24]	2D	No	No	Yes	Joints	Yes	No	Yes
Xiang et al. (2011) [12]	3D	Yes	No	No	Joints	No	Yes	No
Halloran et al. (2010) [25]	2D	No	No	Yes	Joints	Yes	Yes	No
Mahboobin et al. (2010) [26]	2D	No	No	Yes	Joints	Yes	Yes	No
Remy and Thelen (2009) [13]	3D	Yes	No	Yes	Markers/joints	No	No	No
Kim et al. (2008) [14]	3D	Yes	No	No	N/A	No	Yes	No
Fregly et al. (2007) [15]	3D	Yes	Yes	No	Markers	No	Yes	Yes
Thelen and Anderson (2006) [16]	3D	Yes	No	Yes	Joints	No	No	No
Arnold et al. (2005) [17]	3D	No	No	Yes	Joints	Yes	No	No
Anderson and Pandy (2001) [18]	3D	No	No	Yes	Joints	Yes	Yes	No

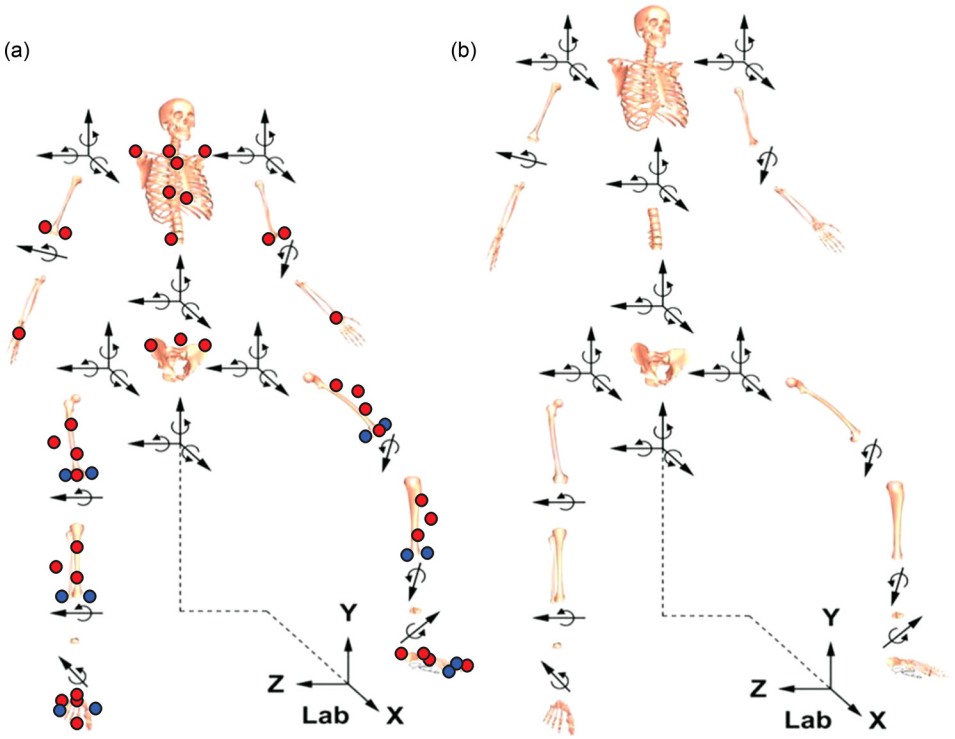

Fig. 1 Schematics of the 29 DOF one back joint (*a*) and 29 or 32 DOF two back joint (*b*) full-body gait models used to evaluate the enhanced REA. The static markers for both the right and left legs are the medial and lateral knee, the medial and lateral ankle, and the medial and lateral toe joint markers. Dark blue circles indicate static markers removed after the static trial and light red circles indicate dynamic markers.

marker positions closely. To accomplish these goals, the algorithm uses the matrix pseudo-inverse to solve an underdetermined linear system of six whole-body dynamics equations (in which no net joint forces or moments appear) for 32 generalized acceleration variations ($\delta\ddot{q}$). These variations define the minimum magnitude change in the model's generalized accelerations ($\ddot{q}$) away from a desired set of generalized accelerations ($\ddot{q}^*$):

$$\ddot{q} = \ddot{q}^* + \delta\ddot{q} \tag{1}$$

The desired generalized accelerations are determined by applying an optimal feedback strategy to experimental joint motion data

$$\ddot{q}^* = \ddot{q}' + k_v(\dot{q}' - \dot{q}) + k_p(q' - q) \tag{2}$$

In this equation, k_p is a feedback gain on joint position error, k_v is a feedback gain on joint velocity error, q and $\dot{q}$ are the model generalized coordinate and velocity values, respectively, and q', $\dot{q}'$, and $\ddot{q}'$ are the experimental generalized coordinate, velocity, and acceleration values, respectively, derived from an initial inverse kinematics analysis. At the initial time frame, Eq. (2) and the initial model state $(q, \dot{q})$ are used to calculate the initial desired generalized accelerations ($\ddot{q}^*$), which in turn via Eq. (1) are used in the six whole-body dynamics equations to solve for the generalized acceleration variations ($\delta\ddot{q}$). The model generalized accelerations ($\ddot{q}$) (which will satisfy the whole-body dynamics equations exactly) are then updated based on Eq. (1) and numerically integrated, and the process is repeated for each subsequent time frame. Using the initial model state as design variables, an optimization repeats the entire process until errors between experimental and model marker positions are minimized.

To improve the ability of the original REA to match measured marker positions accurately, we investigated four modifications to the algorithm (Fig. 2). First, to improve foot marker tracking, we adjusted the marker tracking weights in the original REA cost function. The original weights were 5 for the dynamic lower body markers and 1 for the remaining markers [13]. We increased the weight on the three hindfoot markers to 100 to track the feet closely and the weight on the shoulder markers to 10 to prevent the trunk from falling over. We chose large foot marker weights to encourage achievement of hindfoot marker errors within 1 mm of the best-case solution produced when each hindfoot was treated as an isolated free body [29]. All other marker weights were less than 10 (see below) and manually chosen to maintain hindfoot marker errors within 1 mm of the best-case solution for the four tasks used in this study. Since the foot was modeled as a single rigid body, we only tracked the motion of the three hindfoot

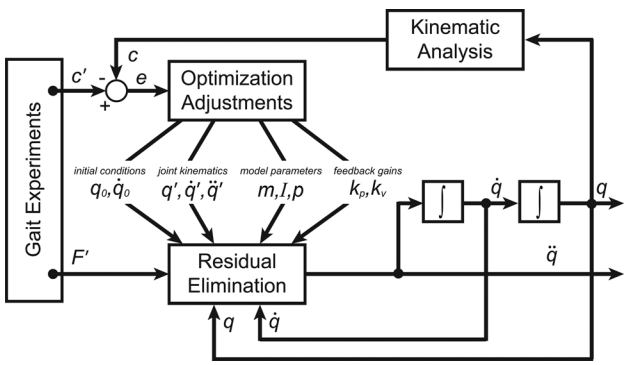

Fig. 2 Schematic of our enhanced REA (modified from [13]). Experimental marker coordinates c' and ground reactions F' are input to the algorithm. The algorithm adjusts model initial conditions q_0 and $\dot{q}_0$, assumed experimental joint kinematics q', $\dot{q}'$, $\ddot{q}'$, model inertial and joint parameter values m, I, p, and optimal feedback gains k_p and k_v. Generalized accelerations $\ddot{q}$ calculated by residual elimination are numerically integrated to determine corresponding generalized speeds $\dot{q}$ and coordinates q. An inverse kinematics analysis is then used to calculate corresponding model marker coordinates c, which are compared with experimental marker coordinates at the same time frame.

markers and set the toe marker weight to zero. Marker weights were the only manual modifications made to the algorithm. The remaining modifications were automated within the enhanced REA optimization methodology.

Second, to account for errors in the experimental q', $\dot{q}'$, and $\ddot{q}'$ curves being used in Eq. (2), we allowed our REA to adjust these curves automatically. The experimental q' curves have errors since they are obtained from an initial inverse kinematics analysis using noisy marker data, and the experimental $\dot{q}'$ and $\ddot{q}'$ curves have errors since they are produced by differentiating inaccurate q' curves [30]. We parameterized the initial q' curves using a combination of polynomial and Fourier coefficients [31], thereby allowing us to calculate the associated $\dot{q}'$ and $\ddot{q}'$ curves analytically. This approach has worked well for previous studies [10,32,33]. We then treated these coefficients as design variables to be adjusted by the optimization. We used 20 coefficients to parameterize each of the 29 or 32 q' curves as follows:

$$\ddot{q}_j = a_0 + a_1 t + a_2 t^2 + a_3 t^3 + \sum_{k=1}^{8} a_{(2k+2)} \cos(k\omega t) + \sum_{k=1}^{8} a_{(2k+3)} \sin(k\omega t) \quad (3)$$

where $\ddot{q}_j$ are the 29 or 32 acceleration curves, a_0 through a_{19} are the polynomial and Fourier coefficients, t is the time, and ω is the angular frequency. This parameterization method essentially smoothes the kinematic trajectories being tracked by the feedback controller but not the marker coordinates being tracked by the cost function. This modification added 580 or 640 design variables (depending on how the back joint was modeled) to the optimization, which significantly increased computation time. Since these kinematic parameterization coefficients remained design variables during optimization of each trial, their values differed between trials.

Third, to improve the performance of the feedback control system, we changed the single k_p gain in the original formulation into nine k_p gains adjusted by the optimization, with each value controlling a different set of generalized coordinates. In the original REA, the position gain was 100 and the velocity gain was 20 for all DOFs. In our modified formulation, we used an initial guess of 100 for each of our nine position gains: three pelvis translations (1 gain), three pelvis rotations (1 gain), all back rotations (1 gain), all arm DOFs (1 gain), 2 DOFs for each ankle (4 gains), and the remaining lower body DOFs (1 gain). We defined the associated k_v gains by

$$k_v = 2\sqrt{k_p} \quad (4)$$

which drives the feedback error terms to zero in a critically damped manner [34].

Fourth, to improve marker tracking while maintaining zero pelvis residual loads, we included lower body joint and inertial parameter values as additional design variables in the optimizations. We allowed the masses and inertias of each body segment to be adjusted by up to 10% from their initial values calculated from the literature [35]. We also allowed joint parameter values for the lower body segments, as well as center of mass locations for all segments, to be adjusted by up to 5 mm or 5 degrees from their initial values calculated from the literature [35]. None of these limits were reached in any of our optimizations.

Enhanced REA Evaluation. We evaluated our enhanced REA using experimental gait data collected from a single healthy subject (male, age 46, height 1.7 m, weight 69 kg) who performed four gait tasks: walking, marching, running, and bounding. The study was institutional review board approved, and the subject gave informed consent prior to testing. Surface marker positions were measured using a 14-camera Vicon motion capture system (Vicon Motion Systems, Inc., Lake Forest, CA), while ground reaction forces and moments were measured using three Bertec force plates (Type 4060-08, Bertec Corp., Columbus, OH). The data collection protocol and marker set were identical to a previous study [15]. Four markers were placed on each foot (including a toe marker), three on each shank and thigh, three on the pelvis, four on the torso, and one on each elbow and wrist. Markers on the same body segment were not part of a rigid cluster. This marker set permitted tight tracking of lower body segment motions and less stringent tracking of upper body segment motions. To facilitate REA evaluation, we collected five trials of each gait pattern with clean strikes on all three force plates.

Using these data and the three variations of our full-body gait model, we followed a four-step process to evaluate our enhanced REA. First, we calibrated the joint and inertial parameter values in each model using data from a single walking trial. From the five recorded walking trials, the one with the walking speed closest to the mean of all five trials was chosen for this step. As part of this step, we also manually selected an initial set of marker weights (pelvis: 8, thigh: 2.8, shank: 1.2, toe: 0, arms: 3, trunk: 0.2, and xiphoid: 1.5) that tracked hindfoot markers as closely as possible without degrading the tracking of other segment markers. The cost function minimized marker tracking errors, changes in joint and inertial parameter values away from their initial values, and differences between the initial and final state (i.e., near-periodic motion).

Second, using the calibrated joint and inertial parameter values from the first step, we manually determined one refined set of marker weights for all three models (pelvis: 9, thigh: 3.8, shank: 1.7, toe: 0, arms: 4, trunk: 0.2, and xiphoid: 3.2) using data from the same walking trial plus data from a single bounding trial. This bounding trial was chosen in a manner similar to the selected walking trial. We added a bounding trial to this step since bounding was our most dynamic task and we wanted to ensure that the enhanced REA could be used reliably for various locomotion tasks. Marker weights were manually chosen that yielded the lowest root-mean-square (RMS) marker distance errors for the selected bounding trial without significantly degrading the RMS marker distance errors for the selected walking trial. Therefore, there was a trade-off between walking and bounding motions when selecting a single set of marker weights that worked well for all three models. Manual selection of tracking weights is not novel. However, the model can only be calibrated using one trial at a time, and we wanted to choose weights that worked well for all four tasks, which prevented automatic selection of the tracking weights.

Third, the chosen marker weights for all models and joint and inertial parameter values for each model from the first two calibration steps were used to test the enhanced REA on four walking trials excluded from calibration. The cost function for this testing step minimized marker coordinate errors and enforced approximate periodicity. Since gait is a near-periodic motion (i.e., generalized coordinate values over one gait cycle end close to their initial values), we enforced approximate periodicity by including cost function terms that kept the difference between initial and final values within five degrees for rotational coordinates. In addition to walking, we also investigated how well our enhanced REA performed for all five running, four marching (one trial had processing problems), and the four remaining bounding trials.

Fourth, the impact of each enhancement was evaluated individually and in all combinations using the same calibration walking trial with the 29 DOF one back joint model (1BJM) (chosen based on results from the previous step) to determine which enhancement(s) yielded the lowest RMS marker distance errors compared with those produced by the original REA.

Results

The enhanced REA significantly reduced foot marker errors while also reducing overall leg marker errors for walking (Table 2). Compared to the original REA, all segment marker

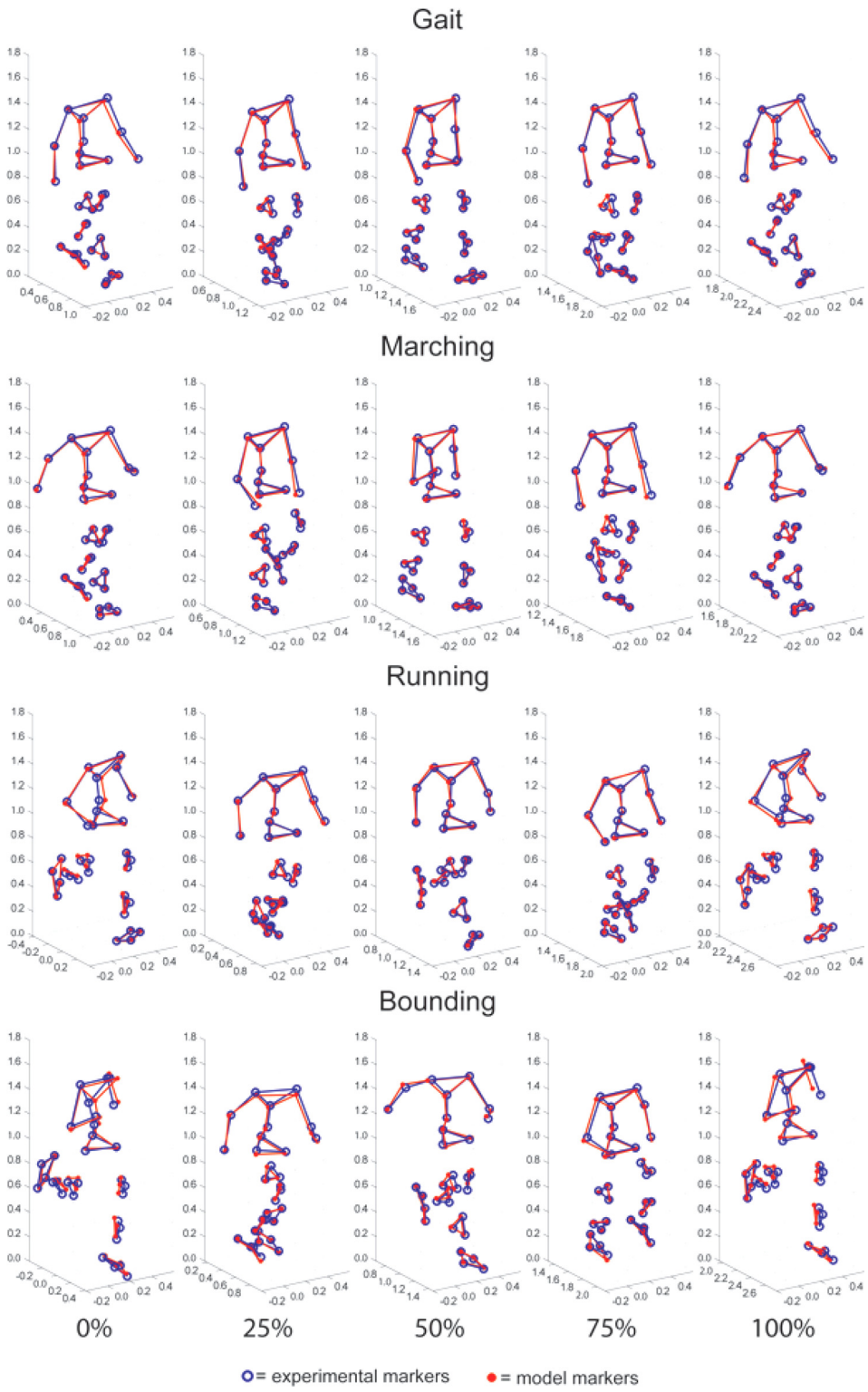

Fig. 3 Comparison between experimental markers (dark blue circles) and model markers (light red dots) for walking, marching, running, and bounding at 0%, 25%, 50%, 75%, and 100% of the locomotion cycle. Units are in meters.

errors were reduced for each of the three gait models except for a slight increase in the trunk marker errors for the 29 DOF two back joint model. The single back joint model yielded the lowest foot marker errors (3.1 mm) compared to the other models (16.0 mm for the original REA, 3.4 mm for 2BJM-D, and 3.3 mm for 2BJM-I) and second lowest overall marker error. While the 32 DOF two back joint model had the highest pelvis marker errors, it produced some of the smallest marker errors for other segments. Despite having the lowest pelvis marker errors, the 29 DOF two back joint model did not improve upper body marker errors and produced the highest overall marker errors of the three models. Foot markers were tracked closely for all three models with RMS errors within approximately 1 mm of the best-case solution produced when each hindfoot segment was treated as an isolated free body. Pelvis residual forces and torques remained below 1×10^{-12} N and 1×10^{-12} Nm, respectively, for all cases.

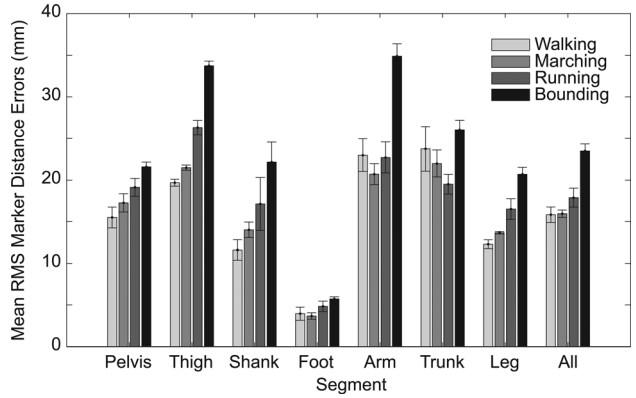

Fig. 4 Enhanced REA RMS marker distance errors over 5 trials for each segment for all locomotion tasks: walking, marching, running, and bounding. Error bars indicate one standard deviation away from the mean. For the marching motion, only four useable trials were available. Leg errors include the pelvis, thigh, shank, and foot. Units are in mm.

Table 2 Mean RMS marker distance errors between the 29 DOF one back joint model using the original REA, 29 DOF one back joint model using the enhanced REA (1BJM), 29 DOF two back joint model (one back joint dependent on the other) using the enhanced REA (2BJM-D), and 32 DOF two back joint model (both back joints independent) using the enhanced REA (2BJM-I). All results are for the calibration walking trial. Units are in mm.

Segment	Original REA	1BJM	2BJM-D	2BJM-I
Pelvis	16.7	14.5	14.3	16.5
Thigh	20.8	19.2	19.0	18.9
Shank	17.9	13.0	12.6	12.5
Foot	16.0	3.1	3.4	3.3
Arm	34.9	19.1	19.3	17.6
Trunk	25.9	21.7	26.1	21.2
Leg	18.0	12.1	12.0	12.3
All	22.3	14.8	15.3	14.5

The enhanced REA was also able to eliminate residual loads for the three other gait tasks while minimizing segment marker errors (Fig. 3). The mean RMS marker distance errors were generally higher for the more dynamic motions of running and bounding compared to walking and marching (Fig. 4). Foot markers were tracked closely for all locomotion tasks with considerably lower mean RMS errors compared to all other segments (mean RMS foot marker errors were 4.0 mm for gait, 3.7 mm for marching, 4.8 mm for running, and 5.7 mm for bounding). The pelvis residual forces and torques remained below 1×10^{-11} N and 1×10^{-11} Nm, respectively, for all tasks.

Compared to results from the original REA, all enhancements individually and in combinations reduced RMS foot marker distance errors, though some enhancements increased RMS marker distance errors for other segments (Table 3). For each individual enhancement, the tracked acceleration curve adjustments and the marker weight adjustments yielded the lowest (7.8 mm) and highest (16.3 mm) mean RMS foot marker errors, respectively, while most segment marker errors were lower than those produced by the original REA. For pairs of enhancements, the marker weight and tracked acceleration curve adjustments pairing resulted in the lowest mean RMS foot marker errors (4.1 mm), while the marker weight and feedback gain adjustments pairing resulted in the highest RMS foot marker errors (12.6 mm). The lowest mean RMS foot marker error was achieved by leaving out the feedback gain adjustments from the enhanced REA, though the reduction was trivial (3.07 mm compared to 3.14 mm). All mean RMS segment marker errors were lower for this combination of three enhancements, as well as for the combination of all four enhancements, compared to the original REA.

Discussion

This study evaluated improvements to the original REA developed by Remy and Thelen [13] with the goal of tracking foot marker trajectories more closely and calibrating model parameter values while still maintaining dynamic consistency. Use of all four modifications together resulted in significantly better foot marker tracking as well as somewhat improved leg marker tracking. The omission of feedback gain adjustments yielded slightly better results overall, though the improvements were small, suggesting that feedback gain adjustment was not worth the computational effort. The improved foot marker tracking produced by these enhancements may facilitate the development of predictive gait optimizations that include deformable foot-ground contact models to permit changing foot interactions with the ground.

Compared to results from the original REA, all four modifications resulted in some marker error improvements and slightly altered kinematics (Table 2). To account for inaccuracies in the experimental kinematic data, we allowed the tracked position, velocity, and acceleration curves to vary, resulting in small but reasonable changes in the marker trajectories produced by our

Table 3 Mean RMS marker distance error comparison for individual and combinations of modifications for the enhanced REA. Modifications are defined as: Mod 1 = marker weights, Mod 2 = tracked acceleration curves, Mod 3 = feedback gains, and Mod 4 = model parameters. All results are for the calibration walking trial. Units are in mm. Bold text indicates the two best combinations of modifications.

Segment	Pelvis	Thigh	Shank	Foot	Arm	Trunk	Leg	All
Original REA	16.3	20.0	18.3	18.4	36.7	26.2	18.5	23.2
Mod 1	19.6	21.0	17.7	16.3	40.6	29.6	18.5	24.3
Mod 2	12.7	19.6	15.4	7.8	24.7	25.2	14.1	17.1
Mod 3	14.4	16.7	15.0	12.9	37.6	26.0	14.8	20.6
Mod 4	14.6	16.1	15.4	16.0	28.1	23.7	15.6	19.4
Mods 1 and 2	18.1	23.3	17.0	4.1	24.5	27.6	15.3	18.5
Mods 1 and 3	18.8	16.7	14.0	12.6	33.9	30.7	15.1	20.9
Mods 1 and 4	15.9	14.3	10.0	7.8	23.4	23.5	11.4	15.6
Mods 2 and 3	12.8	19.5	15.5	8.2	24.8	25.4	14.2	17.4
Mods 2 and 4	11.0	17.9	14.0	6.8	21.3	22.1	12.6	15.4
Mods 3 and 4	11.9	14.1	12.3	10.2	32.5	23.5	12.1	17.6
Mods 1-3	19.0	21.7	15.0	4.2	27.4	29.0	14.4	18.6
Mods 1-2,4	**14.3**	**19.3**	**13.2**	**3.1**	**17.8**	**21.6**	**12.2**	**14.7**
Mods 1,3-4	17.3	14.1	10.3	8.3	22.7	25.6	11.8	16.0
Mods 2-4	11.0	17.9	14.0	6.7	21.7	22.0	12.6	15.4
Mods 1-4	**14.5**	**19.2**	**13.0**	**3.1**	**19.1**	**21.7**	**12.1**	**14.8**

enhanced REA. The optimized kinematics showed slightly more rotation of the pelvis, back, and shoulders to reduce overall marker errors (Fig. 3). Regardless of which model was used, the enhanced REA algorithm resulted in lower marker errors for all segments (Table 2), with the only exception being the trunk marker error for the 29 DOF two back joint model.

Somewhat surprisingly, splitting the trunk into two segments did not significantly improve marker tracking errors compared to a single-segment trunk (Table 2). Adding a joint at the T8-T9 level may not have been the best way to test the benefits of a second back joint in the model, as there is not much flexibility in the rib cage. Alternatively, choosing the second back joint at the T12-L1 level could potentially be more useful because the back has more flexibility in the lumbar region. With a second back joint at the T8-T9 level, marker tracking errors for all segments were comparable between our three models, with a few exceptions. The 29 DOF two back joint model yielded the highest trunk marker errors (even compared to the original REA model), while the 32 DOF two back joint model yielded the highest pelvis and lowest arm marker errors. However, the free rotational motion of the lower trunk segment in the 32 DOF model resulted in a non-unique solution. Overall, the reduced complexity of the one back joint model was sufficient for improving both foot marker tracking and tracking of markers on other segments.

Our improvements to the original REA came at a significant computational cost. The original REA formulation simultaneously adapts only the initial positions and velocities of the 29 generalized coordinates (total design variables = 58). The enhanced REA formulation has 866 design variables that also account for parameterization of joint kinematics, feedback gains, and joint and inertial parameters. For the original REA, the time required to process one walking trial using the 29 DOF one back joint model was 9 min. In contrast, for the 29 DOF one back joints, 29 DOF two back joints, and 32 DOF models, the enhanced REA using all four modifications required 1.9 hrs, 3.4 hrs, and 2.9 hrs, respectively, to process the same walking trial. Not only were results for the one back joint model sufficient in terms of accuracy, but the computation time was much lower compared to both of the two back joint models.

Our analysis of each REA enhancement performed separately and in combinations (Table 3) revealed that adjustment of the tracked kinematic curves had the most impact on reducing foot marker errors. Use of two modifications together led to improvements compared to the original REA but did not achieve the desired level of accuracy for the foot markers. Surprisingly, the marker weight adjustments were involved in the lowest (with tracked kinematic curve adjustments) and highest (with feedback gain adjustments) foot marker errors for combinations of two adjustments, which may suggest greater importance of the tracked acceleration curve adjustments and lesser importance of the feedback gain adjustments. Use of groups of three modifications, specifically all but the feedback gain adjustments, resulted in the best overall marker tracking errors. Feedback gain adjustments appeared to affect the solution only at the level of numerical noise. Therefore, the best approach appears to be a combination of manual adjustments to marker weights, automatic adjustments to tracked kinematic curves, and automatic adjustments to model parameter values if the goal is to reduce foot marker errors without increasing marker errors for other segments.

This study was not without limitations. Our focus was on the development of the enhanced REA approach and showing that it works for other tasks while reducing RMS foot marker errors for walking and eliminating pelvis residual forces and torques. Therefore, we only tested the algorithm on one subject. While we have not tested our approach on subjects with neurological or musculoskeletal impairments, our results provide no indication that similar improvements would not be attained for a subject with impairments or for a different healthy subject. In addition, our walking model is based on principles of rigid multibody dynamics and did not account for soft tissue deformations explicitly. However, such deformations were accounted for implicitly by the use of best-fit model parameter values.

With these three modifications, the enhanced REA may be useful for gait optimizations that utilize deformable foot-ground contact models, where foot position and orientation are important for modeling foot–floor interaction. The hindfoot of each leg was tracked to within 1 mm of the best-case errors, sufficient for incorporating a multi-segment deformable foot-ground contact model into the full-body model. By allowing the optimizer to modify the tracked joint acceleration curves while minimizing a clinically useful cost function (e.g., minimize the peak knee adduction moment), the enhanced REA may be able to predict new gait patterns for investigating novel rehabilitation strategies. These findings also demonstrate that greater back flexibility may not improve marker tracking significantly in computational gait models, suggesting that a one back joint model is sufficient for simulating gait patterns that do not involve large trunk motions.

Acknowledgment

This study was funded by NSF grant numbers CBET 1052754 and CBET 1159735.

Nomenclature

DOF = degrees of freedom
Mod = modification
mm = millimeters
N = Newtons
Nm = Newton-meters
REA = residual elimination algorithm
RMS = root-mean-square
1BJM = one back joint model
2BJM-D = two back joint model (dependent degrees of freedom)
2BJM-I = two back joint model (independent degrees of freedom)

References

[1] Murphy, L., and Helmick, C. G., 2012, "The Impact of Osteoarthritis in the United States: A Population-Health Perspective: A Population-Based Review of the Fourth Most Common Cause of Hospitalization in U.S. Adults," Orthop. Nurs., **31**(2), pp. 85–91.
[2] Perry, J., Garrett, M., Gronley, J. K., and Mulroy, S. J., 1995, "Classification of Walking Handicap in the Stroke Population," Stroke, **26**(6), pp. 982–989.
[3] Davie, C., 2008, "A Review of Parkinson's Disease," Br. Med. Bull., **86**(1), pp. 109–127.
[4] Centers for Disease Control and Prevention, 2009, "Prevalence and Most Common Causes of Disability Among Adults—United States, 2005," MMWR, **58**(16), pp. 421–426.
[5] Ostir, G. V., Berges, I. M., Kuo, Y. F., Goodwin, J. S., Fisher, S. R., and Guralnik, J. M., 2013, "Mobility Activity and Its Value as a Prognostic Indicator of Survival in Hospitalized Older Adults," J. Am. Geriatr. Soc., **61**(4), pp. 551–557.
[6] Mutikainen, S., Rantanen, T., Alén, M., Kauppinen, M., Karjalainen, J., Kaprio, J., and Kujala, U. M., 2011, "Walking Ability and All-Cause Mortality in Older Women," Int. J. Sports Med., **32**(3), pp. 216–222.
[7] Blair, S. N., Kohl, H. W., Paffenbarger, R. S., Clark, D. G., Cooper, K. H., and Gibbons, L. W., 1989, "Physical Fitness and All-Cause Mortality. A Prospective Study of Healthy Men and Women," JAMA, **262**(17), pp. 2395–2401.
[8] Bogey, R., and Hornby, G. T., 2007, "Gait Training Strategies Utilized in Poststroke Rehabilitation: Are We Really Making a Difference?," Top Stroke Rehabil., **14**(6), pp. 1–8.
[9] Andriacchi, T. P., 1994, "Dynamics of Knee Malalignment," Orthop. Clin. North Am., **25**(3), pp. 395–403.
[10] Reinbolt, J. A., Haftka, R. T., Chmielewski, T. L., and Fregly, B. J., 2008, "A Computational Framework to Predict Post-Treatment Outcome for Gait-Related Disorders," Med. Eng. Phys., **30**(4), pp. 434–443.
[11] Allen, J. L., Kautz, S. A., and Neptune, R. R., 2013, "The Influence of Merged Muscle Excitation Modules on Post-Stroke Hemiparetic Walking Performance," Clin. Biomech., **28**(6), pp. 697–704.
[12] Xiang, Y., Arora, J. S., and Abdel-Malek, K., 2011, "Optimization-Based Prediction of Asymmetric Human Gait," J. Biomech., **44**(4), pp. 683–693.
[13] Remy, C. D., and Thelen, D. G., 2009, "Optimal Estimation of Dynamically Consistent Kinematics and Kinetics for Forward Dynamic Simulation of Gait," ASME J. Biomech. Eng., **131**(3), p. 031005.
[14] Kim, H. J., Wang, Q., Rahmatalla, S., Swan, C. C., Arora, J. S., Abdel-Malek, K., and Assouline, J. G., 2008, "Dynamic Motion Planning of 3D Human

Locomotion Using Gradient-Based Optimization," ASME J. Biomech. Eng., **130**(3), p. 031002.
[15] Fregly, B. J., Reinbolt, J. A., Rooney, K. L., Mitchell, K. H., and Chmielewski, T. L., 2007, "Design of Patient-Specific Gait Modifications for Knee Osteoarthritis Rehabilitation," IEEE Trans. Biomed. Eng., **54**(9), pp. 1687–1695.
[16] Thelen, D. G., and Anderson, F. C., 2006, "Using Computed Muscle Control to Generate Forward Dynamic Simulations of Human Walking From Experimental Data," J. Biomech., **39**(6), pp. 1107–1115.
[17] Arnold, A. S., Anderson, F. C., Pandy, M. G., and Delp, S. L., 2005, "Muscular Contributions to Hip and Knee Extension During the Single Limb Stance Phase of Normal Gait: A Framework for Investigating the Causes of Crouch Gait," J. Biomech., **38**(11), pp. 2181–2189.
[18] Anderson, F. C., and Pandy, M. G., 2001, "Dynamic Optimization of Human Walking," ASME J. Biomech. Eng., **123**(5), pp. 381–390.
[19] Higginson, J. S., Ramsay, J. W., and Buchanan, T. S., 2012, "Hybrid Models of the Neuromusculoskeletal System Improve Subject-Specificity," Proc. Inst. Mech. Eng. Part H, **226**(2), pp. 113–119.
[20] Jansen, K., De Groote, F., Duysens, J., and Jonkers, I., 2014, "How Gravity and Muscle Action Control Mediolateral Center of Mass Excursion During Slow Walking: A Simulation Study," Gait Posture, **39**(1), pp. 91–97.
[21] Thompson, J. A., Chaudhari, A. M., Schmitt, L. C., Best, T. M., and Siston, R. A., 2013, "Gluteus Maximus and Soleus Compensate for Simulated Quadriceps Atrophy and Activation Failure During Walking," J Biomech, **46**(13), pp. 2165–2172.
[22] Fey, N. P., Klute, G. K., and Neptune, R. R., 2013, "Altering Prosthetic Foot Stiffness Influences Foot and Muscle Function During Below-Knee Amputee Walking: A Modeling and Simulation Analysis," J. Biomech., **46**(4), pp. 637–644.
[23] Ackermann, M., and van den Bogert, A. J., 2012, "Predictive Simulation of Gait at Low Gravity Reveals Skipping as the Preferred Locomotion Strategy," J. Biomech., **45**(7), pp. 1293–1298.
[24] van den Bogert, A. J., Blana, D., and Heinrich, D., 2011, "Implicit Methods for Efficient Musculoskeletal Simulation and Optimal Control," Procedia IUTAM, **2**(2011), pp. 297–316.
[25] Halloran, J. P., Ackermann, M., Erdemir, A., and van den Bogert, A. J., 2010, "Concurrent Musculoskeletal Dynamics and Finite Element Analysis Predicts Altered Gait Patterns to Reduce Foot Tissue Loading," J. Biomech., **43**(14), pp. 2810–2815.
[26] Mahboobin, A., Cham, R., and Piazza, S. J., 2010, "The Impact of a Systematic Reduction in Shoe-Floor Friction on Heel Contact Walking Kinematics—A Gait Simulation Approach," J. Biomech., **43**(8), pp. 1532–1539.
[27] Miller, R. H., Brandon, S. C., and Deluzio, K. J., 2013, "Predicting Sagittal Plane Biomechanics That Minimize the Axial Knee Joint Contact Force During Walking," ASME J. Biomech. Eng., **135**(1), p. 011007.
[28] Reinbolt, J. A., Haftka, R. T., Chmielewski, T. L., and Fregly, B. J., 2007, "Are Patient-Specific Joint and Inertial Parameters Necessary for Accurate Inverse Dynamics Analyses of Gait?," IEEE Trans. Biomed. Eng., **54**(5), pp. 782–793.
[29] Söderkvist, I., and Wedin, P. A., 1993, "Determining the Movements of the Skeleton Using Well-Configured Markers," J. Biomech., **26**(12), pp. 1473–1477.
[30] Cahouët, V., Luc, M., and David, A., 2002, "Static Optimal Estimation of Joint Accelerations for Inverse Dynamics Problem Solution," J. Biomech., **35**(11), pp. 1507–1513.
[31] Nagurka, M. L., and Yen, V., 1990, "Fourier-Based Optimal Control of Nonlinear Dynamic Systems," ASME J. Dyn. Syst. Meas. Control, **112**(1), pp. 17–26.
[32] Koh, B. I., Reinbolt, J. A., George, A. D., Haftka, R. T., and Fregly, B. J., 2009, "Limitations of Parallel Global Optimization for Large-Scale Human Movement Problems," Med. Eng. Phys., **31**(5), pp. 515–521.
[33] Fregly, B. J., 2009, "Design of Optimal Treatments for Neuromusculoskeletal Disorders Using Patient-Specific Multibody Dynamic Models," Int. J. Comput. Vis. Biomech., **2**(2), pp. 145–155.
[34] Greenwood, D. T., 1988, *Principles of Dynamics*, 2nd ed., Prentice-Hall, Upper Saddle River, NJ.
[35] de Leva, P., 1996, "Adjustments to Zatsiorsky-Seluyanov's Segment Inertia Parameters," J. Biomech., **29**(9), pp. 1223–1230.